PROTEINS
STRUCTURE ■ FUNCTION ■ BIOINFORMATICS

Structural insight into the UNC-45–myosin complex

Filip Fratev,[1*] Svava Ósk Jónsdóttir,[2] and Ilza Pajeva[3]

[1] Micar 21 Ltd., 1470 Sofia, Bulgaria

[2] Department of Toxicology and Risk Assessment, Technical University of Denmark, National Food Institute, DK-2860 Søborg, Denmark

[3] Institute of Biophysics and Biomedical Engineering, Bulgarian Academy of Sciences, 1113 Sofia, Bulgaria

ABSTRACT

The UNC-45 chaperone protein interacts with and affects the folding, stability, and the ATPase activity of myosins. It plays a critical role in the cardiomyopathy development and in the breast cancer tumor growth. Here we propose the first structural model of the UNC-45–myosin complex using various *in silico* methods. Initially, the human UNC-45B binding epitope was identified and the protein was docked to the cardiac myosin (MYH7) motor domain. The final UNC45B–MYH7 structure was obtained by performing of total 630 ns molecular dynamics simulations. The results indicate a complex formation, which is mainly stabilized by electrostatic interactions. Remarkably, the contact surface area is similar to that of the myosin-actin complex. A significant interspecies difference in the myosin binding epitope is observed. Our results reveal the structural basis of MYH7 exons 15–16 hypertrophic cardiomyopathy mutations and provide directions for drug targeting.

Proteins 2013; 00:000–000.

Key words: UNC-45; myosin; molecular dynamics; docking; HCM.

INTRODUCTION

Myosins comprise a family of ATP-dependent motor proteins that play a fundamental role in cellular processes such as muscle contraction, cytokinesis, vesicle transport, and cell motility.[1] Many diseases are linked to the alteration in functions of these proteins. Mutations in the human cardiac myosin heavy chain (MYH7) are known to be responsible for several cardiomyopathies, in particular the hypertrophic cardiomyopathy (HCM).[2] Nearly 45% of the known HCM mutations are found in MYH7, but the role of most of them is unclear.[2] Understanding the role of the mutations is important for discovery of a drug for treating this disease.

UNC-45 co-chaperone proteins are known to be necessary for myosin folding and/or accumulation, thick filament assembly and muscle function.[3–5] The UNC-45B variant of the protein, typical for vertebrates only, has 44% sequence similarity to UNC-45A and is expressed predominantly in cardiac and skeletal muscles.[6] Very recently it has been shown that UNC-45B plays a crucial role in stabilization of the cardiac myosin, organization of myofibrillar heart contractility, and prevention of cardiomyopathies.[7] The latter is the most common inherited heart disease in humans and pets, and one of the main reasons of sudden death of young athletes.[8] Dilated cardiomyopathy was associated with UNC-45B deficiency and was mimicked in a myosin knockdown experiment, indicating that UNC-45 can be a possible drug target for cardiomyopathy treatment.[7]

Additionally, it has been recently shown that UNC-45 plays a critical role in the breast cancer tumor growth. This protein became an attractive object for treatment of breast cancer due to the observed overexpression in tumor cells, which was four times higher than in normal cells.[9]

Numerous myosin X-ray structures have been resolved. The atomic structures of chaperone proteins with UNC-45/CRO1/She4p (UCS) binding domains have recently been obtained for two species, namely the fungal She4p and the *Drosophila* UNC-45.[10,11] The binding epitopes of yeast myosins, such as Myo3p and Myo4p, were identified and located at the C-Terminal region of the myosin head, but the UNC-45 epitope was not specified. However, it is known that myosin binds to the UCS domain of UNC-45.[10–12] Moreover, most of the experi-

Additional Supporting Information may be found in the online version of this article.

*Correspondence to: Filip Fratev, Micar 21 Ltd., Persenk 34b, 1470, Sofia, Bulgaria. E-mail: fratev@clbme.bas.bg.

Received 4 October 2012; Revised 6 January 2013; Accepted 31 January 2013
Published online 14 February 2013 in Wiley Online Library (wileyonlinelibrary.com).
DOI: 10.1002/prot.24270

mentally identified mutations in *Caenorhabditis elegans* and *Schizosaccharomyces pombe* that affect the ability of UCS proteins to function as essential modulators of myosin activity were identified in the UCS domain.[11,12]

It has been shown that UNC-45 binds both, the molecular chaperone Hsp90 and myosin. The binding occurs via different domains and Hsp90 has an inhibitory role in respect to the UNC-45 action presuming that UNC-45 binds directly to the myosin head.[5] In this way UNC-45 regulates the myosin-actin interactions since its binding to the myosin head is essential for efficient *in vitro* actin binding.[5] Previously She4p interactions with myosin have been mapped on all five yeast myosins. The She4p interacting region of Myo4p has been reported to cover residues 531–631.[12] Further a finer mapping of this interaction has been performed and a 27-residue long segment of Myo4p (residues 561–587) has been specified.[10] This segment is highly conserved, not only in all five yeast myosins, but also in the subfamilies of identified myosins, including the human cardiac myosin.[10] It has been found that this Myo4p segment binds to UCS with a binding affinity of approximately 1 μM.[10] Data for the whole myosin-UNC-45B complex, obtained very recently by various experimental techniques, show an apparent K_d value of 1.3 μM, thus confirming that the UNC-45B interacts robustly with the myosin motor domain.[5,13] Further, the binding site of myosin has been refined by methods different from the above mentioned techniques and it has been concluded that the SH1 and SH2 segments of the motor domain might be directly or indirectly involved in the UNC-45B interactions.[13] However, it should be noted that disparate functions have been proposed for UCS. The protein was first described as a chaperone for myosin folding.[14–16] Subsequent reports invoked UCS in protecting myosin from degradation[17,18] and in enhancing the binding of the motor domain of myosin to actin filaments.[5,18,19]

In this study, which we base on analysis of X-ray data, we suggest that a UCS dimer of UNC-45B links two myosin motor domains and thereby functions as one of the determinants for step size of myosin on actin filaments.[10] Indeed the latter requires formation of a UNC-45–myosin complex. Thus, an atomic model of the UNC-45–myosin complex is primarily needed to answer several important questions: (1) where is the specific UCS binding region of UNC-45 and how does it interact with myosin? (2) Are there interspecies differences in these interactions? (3) How can the UNC-45B binding be modified in case of phenotypic cardiomyopathy myosin mutants and how does it reflect on the myosin-actin binding? To answer these questions, in this work we concentrated on modeling the wild-type complex features by various *in silico* approaches. We aimed at gaining a structural insight into the complex at an atomic level. Our results indicate a formation of a complex stabilized mainly by electrostatic interactions with a contact surface area similar to that of the myosin-actin complex. We also observed a significant interspecies difference in the myosin binding epitope and propose a structural basis of MYH7 exons 15–16 hypertrophic cardiomyopathy mutations.

MATERIALS AND METHODS

Homology modeling, preparation of the protein structures and electrostatic potential calculations

The homology models of the human UNC-45B and the motor domain of the cardiac myosin (MYH7) were constructed and refined by the MOE software.[20] Only the motor domain of MYH7 was modelled. For myosin, we used as templates the crystal structures of the chicken myosin S1 (PDB ID: 2MYS) and *Loligo pealei* (PDB ID: 3I5F) due to their high sequence similarity with human MYH7 (>75%). UNC-45B binds to myosin simultaneously with ATP,[3,10] thus we also included *Dictyostelium* myosin structure (PDB ID: 2JHR) for modeling this stage of the ATPase cycle in the human myosin homology model. For the human UNC-45B homology model, the *Drosophila* structure (PDB ID: 3NOW) was used. Further, the side chains of the output models were refined. All settings were set to their defaults. The coordinates of the missing residues of loop-U (571–575 in 2MYS), which are significant for the UNC-45B-myosin complex formation, were transferred directly from the X-ray structure 3I5F, because the resolved portion of the loop-U in 2MYS had an identical conformation. Thus, one can expect a similar conformation in MYH7 too and this has been confirmed later by the deposited X-ray structure of MYH7 (PDB ID: 4DB1). The other gaps present in the 2MYS loop regions were initially modelled based on the myosin *Dictyostelium* structure (PDB ID: 2JHR), which is one of the few fully resolved myosin structures. Residues 205–215 and 627–646 were missing in 2MYS and these loops were *de novo* created and refined. The loop-U only might be involved in the UNC-45B complex formation. All other loops of myosin were far from the myosin binding epitope, and their conformations were therefore unlikely to have any influence. Finally, both the UNC-45B and MYH7 structures were refined by 50 ns-long NPT molecular dynamics (MD) simulations by the Amber 11 package[21] using Amber99SB force field, truncated octahedral box solvated with a 10 Å buffer of TIP3 water molecules and counterions to neutralize the system. Electrostatic potentials were calculated by the APBS software[22] using the default parameters. The measurements of the contact surface area were based on the solvent accessible surface areas (SASA) calculated by the VMD software[23] using the "measure sasa" routine. The sasa-parameter "sradius" was set to 1.4 Å. The H-bond, hydrophobic and ionic interactions were identified in the minimized averaged structure, over the last 10 ns of the

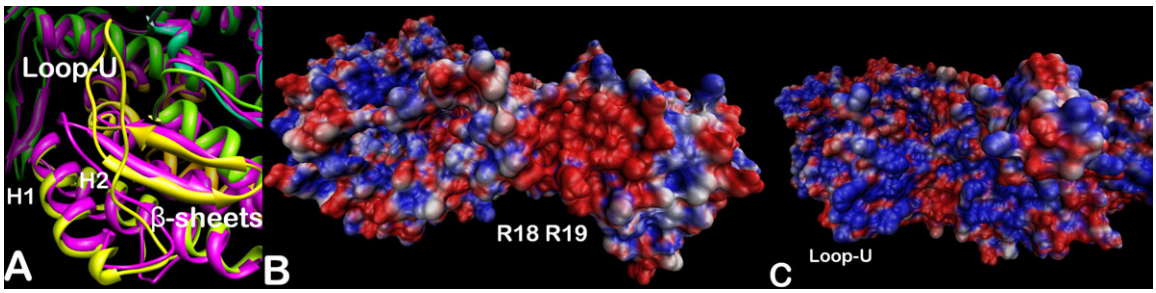

Figure 1

(**A**) Close view of the myosin binding epitope with marked positions of the β-sheets and the loop-U in *Drosophila* (magenta) and *Loligo pealei* (yellow) (see Supporting Information Fig. S8 for the epitope position in the MYH-7 structure). (**B**) The electrostatic potentials of the UCS part of UNC-45B calculated by the APBS method (red is negative, blue is positive). Note that the loop-M and R18-R19 helices are strongly negative. (**C**) The electrostatic potentials of the MYH7 binding epitope fragment calculated by the APBS method (red is negative, blue is positive). Note that the loop-U and the β-sheets are strongly positive.

MD simulation (named Model1, see Supporting Information Fig. S5 and Table S2), by employing the Protein Interactions Calculator (PIC) server.[24]

Epitope prediction of the binding pockets

The ICM ODA web server[25] has been used to predict the UNC-45B binding epitope by ODA (Optimal Docking Areas) approach, in a combination with the Adaptive Poisson-Boltzmann Solver (APBS) calculations. Results were visualised by the ICM-browser. ODA is a method to predict protein-protein interaction sites on protein surfaces. It identifies optimal surface patches with the lowest docking desolvation energy values as calculated by atomic solvation parameters (ASP) derived from octanol/water transfer experiments and adjusted for protein-protein docking. The predictor has been benchmarked on 66 non-homologous unbound structures, and the identified interactions points are correctly located in nearly 80% of the cases.[26]

Binding site identification

The "Site Finder" tool in MOE was employed for identification of the binding pockets in the myosin-UNC-45 complex. The tool uses the methodology of convex hulls which produces pockets invariant to rotation of the atomic coordinates. It treats the set of three-dimensional points by triangulation and associates each resulting simplex with a sphere, coded as "alpha sphere." The radius of the sphere is proportional to the convex hull of the point set. Each sphere is classified as either "hydrophobic" or "hydrophilic" depending on whether the sphere is a good HB point in the receptor. Hydrophilic spheres not close to hydrophobic ones are eliminated as they generally correspond to water sites. The generated pockets consist of one or more alpha spheres, and at least one is hydrophobic. The default settings were used.

Protein-protein docking

Initial orientation of the UNC-45B to MYH7 was obtained by HEX 6.3 docking software.[27] Protein-protein docking was performed by the HADDOCK web server using the default settings.[28] The significant interspecies difference in the loop-U size and conformation considered to be critical for the UNC-45B binding to the human cardiac myosin was the reason that we did not benefit from the X-ray *Drosophila* structure (PDB ID: 3NOW). Instead, we used the MYH7 structure generated by homology modeling for the docking procedure (see Results and Discussion paragraph). Besides, a very recent study showed that the calculated free energy of binding using a homology modelled structure generated by multiple templates does not show any significant differences compared with those obtained using the X-ray structure.[29] We used the experimentally detected myosin binding epitope[10] for the yeast myosin Myo4p that corresponded to residues 631–672 in MYH7. Residues that were obtained by the ODA approach, were considered to be most likely involved in protein-protein interactions. Thus residues from the loop-M and helixes 18–19 [Figs. 1(C) and 2] were selected as the binding epitope of UNC-45B. The remaining residues were included in the class of surrounding non-interacting residues.

A HADDOCK score was defined to rank the structures after each docking stage. It is a weighted sum of intermolecular electrostatic (Elec), van der Waals (vdW), buried surface area (BSA), desolvation (Dsolv), and AIR energies: rigid-body score = $1.0 \times$ Elec + $1.0 \times$ vdW - $0.05 \times$ BSA + $1.0 \times$ Dsolv + $1.0 \times$ AIR, final score = $1.0 \times$ Elec + $1.0 \times$ vdW + $1.0 \times$ Dsolv + $1.0 \times$ AIR. The AIR term represents the so-called Ambiguous Interaction Restraints (AIRs) used to drive the docking process. An AIR is defined as an ambiguous distance between all residues shown to be involved in the interaction. As an output the top 10 clusters, each containing 10 docking solutions, were obtained and the cluster with the lowest energy was selected.

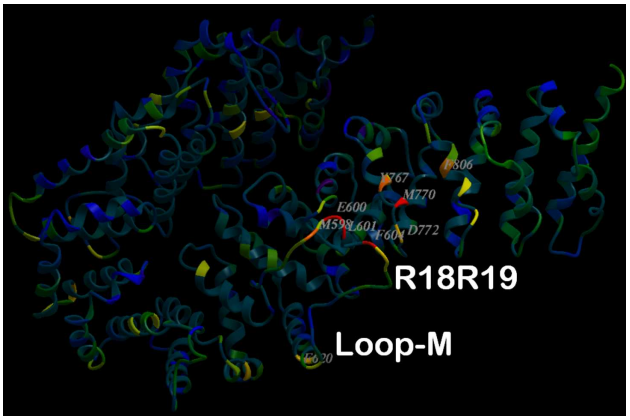

Figure 2

The binding epitope of *Drosophila* UNC-45 identified by ODA analysis. Similar results were obtained for the human UNC-45B (see Supporting Information Fig. S4). The residues marked in red and yellow are the most likely to be involved in protein-protein interactions. [Color figure can be viewed in the online issue, which is available at wileyonlinelibrary.com.]

Molecular dynamics

Molecular dynamics and free energy Molecular Mechanics Poisson-Boltzmann/Surface Area (MM-PBSA) computations were carried out using the Amber 11 suite of programs[21] and the Amber99SB force field. The ATP molecule, Mg^{2+} ion and the five water molecules in the nucleotide pocket were kept. The commonly adopted parameters and charges for the ATP molecule were employed.[30] As input structures we used those obtained by docking analysis and refined, as described above, by 50 ns-long NPT MD simulations. A truncated octahedral box of TIP3 water molecules of 12 Å dimension in each direction and counterions were added to obtain the final solvated system, which consisted of nearly 240,000 atoms. Initially, the systems were minimized for 10,000 steps. Further, a simulated annealing (SA) procedure was applied to the identified myosin binding epitope and the loop-M of UNC-45B [see Figs. 1(A) and 2 in Results and Discussion section for more details). The remaining parts of the proteins were harmonically constrained by a force constant of 5 kcal/mol/Å^2. We run more than 20 independent MD simulations in a NVT ensemble, heating selected protein regions up to 600 K and 800 K for periods between 20 ns and 50 ns. The heating step required a deep sampling due to the potential significant conformational changes during the protein-protein binding, the high energy barriers and the large size of the system.

Several MD runs were performed (see Results and Discussion section for more details). As a first step two independent 50 ns simulations at 600 K were done to study the possible conformations of the UNC-45B loop-M. Next, to investigate interactions between selected structural elements of the complex, we run 16 independent 20 ns-long simulations at 600 K and 800 K (one at 600 K with fully restricted H1 and H2 helices, 8 at 600 K with partially restricted H1 and H2 and 7 at 800 K with fully restricted H1 and H2). Each of these simulations was followed by a total of 70 ns cooling and equilibrations in a NVT ensemble. Then the two lowest energy complexes were selected from each of the heating schemes above (600 K and 800 K) and two unrestricted 50 ns-long production runs at 310 K in a NPT ensemble were employed for these complexes. The finally selected complex was confirmed by two independent 15 ns- and 25 ns-long simulations. Thus, the combined length of the performed MD simulations was over 630 ns. Temperature regulation was done by using a Langevin thermostat with collision frequency of 2 ps^{-1}. The time step of the simulations was 2 fs with a non-bonded cut-off of 10 Å using SHAKE algorithm[31] and the PME method.[32] The calculation of the residues contacts between the refined complexes, H-bonds and visualisations were obtained by the Maestro module of the Schrödinger software.[33]

Free energy calculations

Binding free energies of all systems were analyzed using the MM-PBSA approach. The binding free energies (ΔG bind) were computed as:

$$\Delta G\text{bind} = G\ \text{complex} - (G\ \text{protein} + G\ \text{ligand}) \quad (1)$$

$$\Delta G\text{bind} = \Delta G\text{gas} + \Delta G\text{solv} - T\Delta S \quad (2)$$

$$\Delta G\text{gas} = \Delta G\text{ele} + \Delta G\text{vdw} \quad (3)$$

$$\Delta G\text{solv} = \Delta G_{\text{PB}} + \Delta G\text{nonpolar} \quad (4)$$

$$\Delta G\text{nonpolar} = \gamma A + b \quad (5)$$

In Eq. (1) the G ligand term represents the free energy of the UNC-45B protein, whereas the G protein term is the free energy of myosin, and G complex is the energy of the UNC-45–myosin complex. The sum of the molecular mechanical energies, ΔG gas, was divided into contributions from the electrostatic potential (ΔG ele), and the van der Waals (ΔG vdw) potential [Eq. (3)]. The solvation free energy (ΔG solv) was composed of a polar (ΔG_{PB}) and a nonpolar (ΔG nonpolar) solvation free energy [Eq. (4)]. All energies were averaged along the MD trajectories. Both, the single and multiple trajectory approach were applied to estimate the energies. In the multiple trajectory approach we used the 50 ns MD simulations of the individual proteins, but as a result the

standard errors were almost 17 times larger than those obtained by the single trajectory approach and a reasonable estimation was not possible. Thus, only the data from the single trajectory approach were used. The advantage of the single approach over the multiple one is the cancellation of errors that hides the effect of the incomplete sampling. The snapshots of each system were sampled from the last 10 ns single trajectory with an interval of 10 ps, that is, 1000 snapshots. ΔG gas was obtained using Amber 11 sander module, and estimation of ΔG_{PB} was conducted with a built-in module PBSA in Amber 11. G nopolar was determined from Eq. (5), where A is the solvent-accessible surface area estimated using Molsurf program, which is a part of Amber 11 suite programs, with a solvent probe radius of 1.4 Å; γ and b are empirical constants set to 0.0072 kcal mol^{-1} Å^{-2} and 0.92 kcal/mol, respectively. The entropy term [$T\Delta S$ in Eq. (2)] was neglected due to the large size of the system that made this calculation impractical. Thus only the enthalpy contribution to the binding was determined by this method, and to clarify this we used the term ΔH and not ΔG when reporting our results.

pH-dependent calculation of the free energy

These calculations were performed using the web-based pH-dependent Electrostatic calculation of Free Energy of Proteins.[34] It was possible to estimate not only the electrostatic part [ΔG_{el} (pH)], but also the total free energy [ΔG_{tot}(pH)] which includes all pH-independent/"hydrophobic"/contributions [ΔG_h].

$$[\Delta G_{tot}(\mathrm{pH})] = [\Delta G_{el}(\mathrm{pH})] + [\Delta G_h] \qquad (6)$$

For the calculation of ΔG_{tot} (pH) term one needs only the correct three-dimensional-atomic structure of the protein. The calculation of [ΔG_{el} (pH)] is preceded by calculation of the Z (pH) function—net-charge as a function of pH (i.e. the potentiometric titration curve). This approach has been tested on many proteins with experimentally determined stability ΔG_{exp} (pH) at fixed pH values.[35] The [ΔG_h] term was obtained by the following considerations. If the reversible binding of P to L (both P and L are proteins/polypeptides) producing a PL complex and the equilibrium constant $K = [PL]/[P] \times [L]$ (at standard conditions) determines the affinity of L to P ($\Delta G_{aff,L}$ in kcal/mol), then the affinity can be defined by the difference:

$$[\Delta G_{aff,L}(\mathrm{pH})] = [\Delta G_{tot,PL}(\mathrm{pH})] - [\Delta G_{tot,P}(\mathrm{pH})] \qquad (7)$$

The same procedure using [ΔG_{el}(pH)] will give the electrostatic part of $\Delta G_{aff,L}$ and from their differences—the pH independent/"hydrophobic"/ part of affinity.

RESULTS AND DISCUSSION

Homology modeling and identification of the UNC-45B binding epitope

Initially homology models of human UNC-45B and cardiac myosin S1 (MYH7) have been constructed. The obtained protein alignments, Ramachandran plots and visualisations are shown in Supporting Information Figures S1–S3. The myosin binding epitope was identified as Myo4p, loop-U, H1, and H2 helices of myosin. The analysis of our sequence alignments and those previously performed on the myosin family[36] indicate significant interspecies differences in the myosin binding epitope. The most notable is the insertion of a few additional residues in the loop-U in human cardiac and chicken myosins, compared to the *Dictyostelium* and yeast myosins. This significantly changes the conformation of the myosin binding epitope, forming a "barrier" that limits the UNC-45 access to inside the myosin β-sheets [Fig. 1(A) and Supporting Information Fig. S1). It is worth noting that this difference has not been considered in the previously discussed myosin binding region.[10]

To identify the possible candidates for an UNC-45B binding epitope an electrostatic and ODA calculations have been performed. The electrostatic calculations show that the UCS domain of the human UNC-45B, which is known to interact with myosin, is predominantly negatively charged and forms a negative "hot" spot in the region concentrated at the R18-19 helices and at the long loop between R14 and R15 (loop-M) [Fig. 1(B), see also Fig. 1(A) in Ref. [11]]. On the other hand, the corresponding Myo4p binding epitope in MYH7 is quite positively charged [Fig. 1(C)], a fact that has not been considered so far. This observation indicates that the above mentioned UCS region might be involved in the UNC45-myosin complex, based on electrostatic interactions. Similar approach has been applied recently, and a comparable UNC-45 region has been noted as a potential myosin binding site.[11] According to our analysis, the pocket with the high interspecies sequence similarity, identified as hydrophobic in the *Drosophila* X-ray structure in Ref. [11], is much more negative in human UNC-45B [Fig. 1(B) and Supporting Information Fig. S3).

According to the ICM epitope identifier (ODA analysis) and the above electrostatic analysis, the residues of the loop-M (594–603) and the R18–19 helices were identified as the most likely candidates to be involved in the myosin interactions with UNC-45 (Fig. 2).

It should be mentioned that about 50% of the experimentally identified mutations in *C. elegans* and *S. pombe* that affect the ability of UCS proteins to function as essential modulators of myosin activity, were concentrated at the R18-R20 helices.[11,12] In particular, in *C. elegans* these were: Gly427Glu, Leu559Ser, Glu781Lys, and Leu822Phe. For instance, the genetic and physiological studies of the UNC-45 mutations at position Phe806 identified this

residue as an important modulator of the myosin activity, indicating that Phe806 could be involved in the myosin binding. The significance of this mutation is, however, unclear from the chaperone structure alone.[11] On the other hand, the exons 15–16 HCM myosin mutations, which action is not explained so far, are placed at or around the identified myosin binding epitope. These findings support the electrostatic and ODA calculations above and the identified UNC-45B binding epitope.

Protein-protein docking

Relying on both, our computational results and the experimental data, we focused on the region of the human UNC-45B described above and used it in the protein-protein docking. The experimentally observed myosin binding site residues (631–672) and those identified as a UNC-45 binding epitope (residues from the loop-M and helixes R18–19, Fig. 2) were selected as interacting residues and the remaining residues were considered not to be involved in the interactions. Among the top 10 docking clusters only two had negative scorings (-40.5 ± 20.4 and -11.9 ± 16.8) and the cluster with the most negative score was selected for further consideration. Moreover, this cluster was also in an agreement with the experimentally identified myosin binding epitope.[10] The HADDOCK results indicated a ninefold higher contribution of the electrostatic term than the van der Waals one. Several similar lowest energy conformations were obtained in the lowest energy cluster, and those were visually inspected. In fact, the differences between these solutions were only in the rotation of the UNC-45B loop-M along the common plane, around the myosin binding site in a range of around 30°. Based on the docking solution, in which the loop-M was in the closest contact to the known myosin binding epitope, we speculate that the loop-M flexibility can lead to better contacts between UNC-45A and myosin, in agreement with the experimentally observed myosin binding site.

It should be noted that using protein-protein docking based on the available crystal structures alone and according to simple geometry considerations, the loop-M of UNC-45 was not able to interact strongly with β-sheets residues of myosin and this did not depend on the interacting residues selection. Thus, it becomes evident that the simple rigid protein-protein docking can not fully describe the protein's interactions, but might be used as a starting point for further refinement by optimizing the coordinates of the interacting residues/atoms. Thus, we used SA procedure as a next step in our analysis.

Simulated annealing analysis of UNC-45–myosin binding

To identify the UNC-45 binding mode a series of MD simulations, in particular SA, has been applied. Such an approach is commonly adopted to refine protein-protein docking solutions. The data from 500 ns simulation time during the SA steps, were collected and analysed. The result from the initial two independent 50 ns simulations at 600 K clearly showed that the loop-M of UNC-45B adopted an open conformation, and was able to interact with the β-sheets in the myosin binding site. This chaperone conformation is called here "the UNC-45 open state" (Fig. 3). However, in the run of 20 ns simulation with fully restricted H1 and H2 helices (connected to the beginning of the loop-U in myosin), we observed a partial restriction of the loop-M movement in UNC-45 during the simulations that resulted in a "partially" open state conformation of UNC-45. The chaperon still interacted with some β-sheets residues, but occupied the myosin binding epitope to a lesser extent than in the UNC-45 open state conformation. Thus, we suggest two possible scenarios: either the H1 and H2 helices play a significant role in the complex formation or the energy barrier is too high for reaching an optimal solution. To investigate how these helices influence the complex formation and, in particular, the conformation of the loop-M in UNC-45, we unrestricted consequently H1 and the first half portion of H2 step by step, a few residues at a time, and then run eight simulations heating the complexes up to 600 K for 20 ns. The obtained individual eight conformations were almost identical to the complex with fully restricted H1 and H2. Conversely, when we run seven 20 ns independent simulations heating the system up to 800 K, with restricted H1 and H2, all obtained complexes

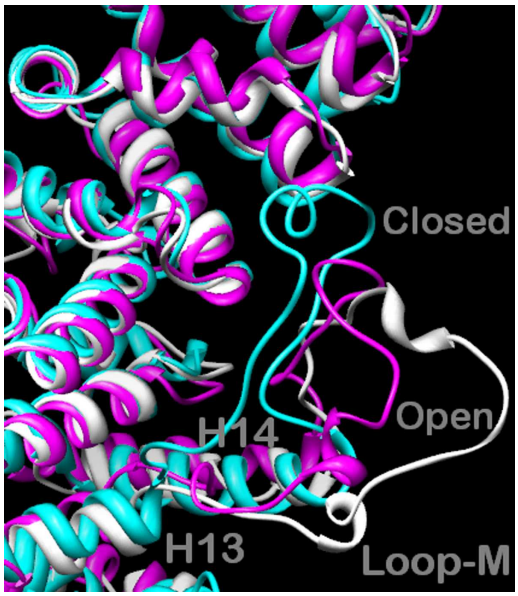

Figure 3

Closed (cyan), partially open (magenta) and open (white) conformational states of the UNC-45B loop-M obtained by simulated annealing method. The positions of the H13 and H14 helices are shown as well. [Color figure can be viewed in the online issue, which is available at wileyonlinelibrary.com.]

showed an open state UNC-45B and loop-M fully involved in interactions with both, the loop-U and the β-sheets of the myosin binding site. No unfolding of the unrestricted myosin parts has been observed. Further, the respective lowest energy complex from each of the heating schemes above (600 K and 800 K), were used to finalize the SA analysis by 25 ns cooling via 100 K steps. After 10 ns of equilibration at 310 K, the complexes were used respectively as input structures for fully unrestricted two 50 ns-long MD simulations in a NPT ensemble. As a result, the potential energy of the MD optimized complex obtained for the lowest energy complex from the 800 K SA heating scheme (as an input structure), was significantly lower. This indicates that the energy barrier was too high for the 600 K simulations to reach an optimal solution.

Further, a MM-PBSA analysis was performed to measure the enthalpic part of the free binding energies of these two complexes. The results confirmed those derived by the potential energy comparison (Supporting Information Table S1). Hence, the data showed that H1 and H2 helices were not involved in the complex formation in agreement with the experimental results for the yeast myosin Myo4p.[10] Remarkably, the loop-U of human MYH7 myosin interacted with R18-R20 helices of UNC-45B during all above simulations, and the variation in the simulations was due to different UNC-45B and loop-M conformations. Thus, our results strongly suggest that the loop-U plays a substantial role in the UNC45-myosin complex formation and thereby in the function of the cardiac human myosin. Due to its sequence similarity to other vertebrates, one could expect a similar role of the loop-U in the function of vertebrate myosins. On the other hand, the X-ray structure alignment [Fig. 1(A)] and experimental studies reveal that the loop-U in yeast is not involved in the complex formation, presumably due to its small size. Thus, our results indicate a significant interspecies difference with regard to the UNC-45-mysion complex formation in humans and a simple organism like yeast.

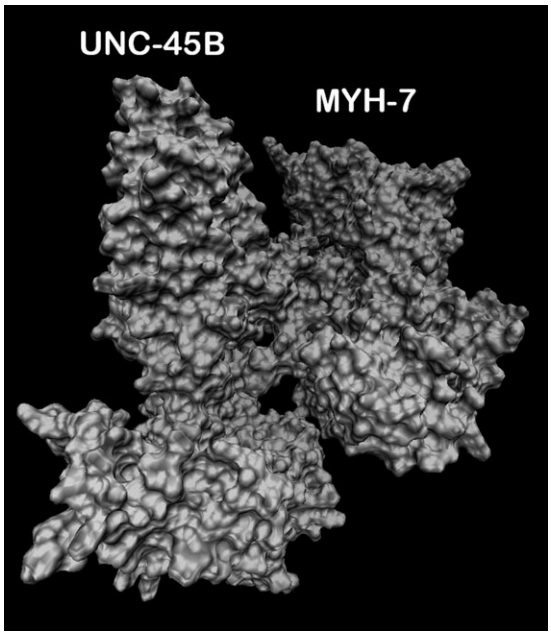

Figure 4

The obtained UNC-45B-MYH7 complex from the simulations performed. See also Figure 5 and Supporting Information Figure S7(A,B) for the secondary structure representation.

Analysis of the identified UNC-45B–MYH7 complex

To validate the obtained lowest energy structure we run additionally two independent 15 ns and 20 ns-long NPT simulations at 310 K (starting from the same complex of the 800 K SA heating scheme as described above). Similar results to the corresponding 50 ns-long MD run were obtained. The RMSD values of the unrestricted MD simulations indicate that the complex underwent significant conformational changes upon binding of the proteins (Supporting Information Fig. S5). A MM-PBSA analysis of these structures was performed and the final UNC-45B-myosin structural complex was generated (see Supporting Information Table S1 for ΔH values). The obtained negative enthalpy value (ΔH) of -103.9 ± 1.06 kcal/mol clearly indicates that this is an energetically favourable protein-protein complex, thus providing an additional support to the above results. However, one should keep in mind that the result does not equal the real binding free energy since we did not estimate the entropy contribution to the binding. The preliminary results of our pH-dependent electrostatic calculation of the free energy of proteins indicate an unfavourable entropy contribution and a total free energy of -8.5 kcal/mol, which is close to the experimental value of K_d = 1.3 μM[14] (Supporting Information Fig. S6). These results confirm the formation of UNC-45B–myosin complex and support a model suggested from the X-ray techniques according to which a UCS dimer of UNC-45 links two myosin molecules at their motor domains and thereby functions as one of the determinants for step size of myosin on actin filaments.[10] Moreover, the orientation of UNC-45 in the UNC-45–myosin complex is in agreement with those suggested previously (see Fig. 4, Supporting Information Fig. S7 and Fig. 6 in Ref. [10]). Further, the results show that the electrostatic interactions are six times greater than the van der Waals ones, demonstrating that the complex formation is stabilized mainly by ionic interactions and H-bonds (Supporting Information Table S1). Remarkably, the contact surface area of the complex was found to be 1598 Å^2, which is close to that obtained for the myosin-actin complex.[37]

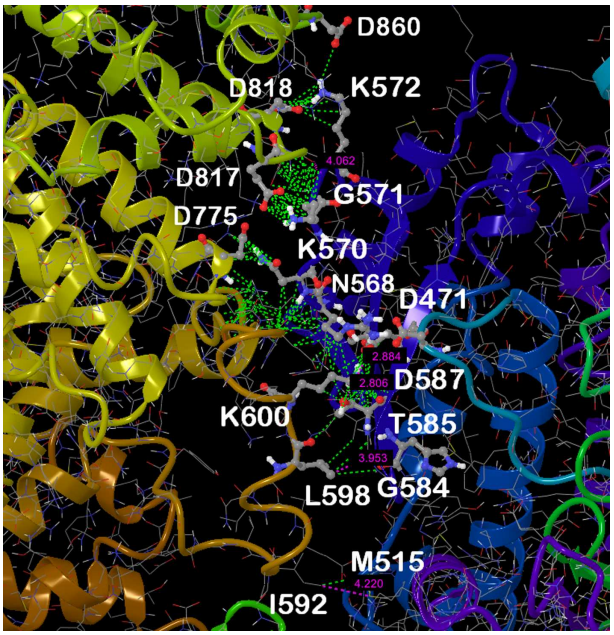

Figure 5

Close view of the contact region and good contacts identified between UNC-45B and MYH7 residues. Note that the positions M515, G584, T585, D587, and G571 in the wild type MYH7 have been experimentally identified as myosin HCM mutations. The atomic contacts (in green) and distances (in magenta) are marked by dotted line. The contacts are defined as good if $C = D_{12}/(R_1 + R_2) > 1.30$ Å, where D_{12} is the distance between atomic centers 1 and 2, and R_1 and R_2 are the radii of atomic centers 1 and 2. [Color figure can be viewed in the online issue, which is available at wileyonlinelibrary.com.]

Figure 5 and Supporting Information Figure S7(A,B) show the obtained UNC-45B-myosin complex and identified atomic contacts. Supporting Information Table S2 presents the types of atomic interactions in the complex and their characteristics. According to our simulations, the loop-U of the myosin interacts with the chaperone R19 helix forming strong H-bonds via a pair of lysine residues and Asn568. The loop-M of UNC-45B interacts with myosin β-sheets residues and the loop-U via a stable H-bond network. In particular one of the loop-M lysines, as it was predicted above, interacts with Asp587, Thr585 and Arg567 in myosin. One can speculate that these interactions might provoke allosteric changes of importance for the myosin ATP binding loop-switch 2 located at the nucleotide pocket. Finally, the loop-U and the loop-M interact with each other. In the UNC-45B open state, R14-R15 helices shifted during the MD simulations. Indeed, the independent simulations showed slight variability in the conformation of the loop-M, but at least one of its lysines (Lys600 and/or 603) interacted with the myosin β-sheets residues. Finally, a more planar UNC-45 structure than those seen in the X-ray was observed in agreement with the experimental data in solution.[11] According to our results interactions with the other parts of myosin are also likely. For instance, the myosin residues in the region Arg696 to Arg705 located in two neighbour helixes are in a close proximity to the loop-M of UNC-45 and could directly or indirectly influence the interactions between the loop and the myosin β-sheets.

Very recently it has been observed that the myosin SH1 and SH2 thiol groups are involved either in a direct binding of the chaperone or in allosteric changes in the motor domain upon the chaperone binding at a different site.[13] Considering that contacts identified here are adjacent to SH1 and SH2 thiol groups, one can conclude that our results are in agreement with these observations.

During the final stage of the manuscript preparation an X-ray structure of MYH7 has been deposited in PDB (ID: 4DB1). The comparison of our homology model to 4DB1 showed that the modelled structure is practically the same (RMSD = 0.8Å of backbones, Supporting Information Fig. S8). This fact gives an additional support for the generated models. Moreover, the loop-U, as predicted above, adopts an extended conformation.

MYH7 exons 15–16 mutations and directions for drug targeting

The above results can help in revealing the structural basis of several hypertrophic cardiomyopathy (HCM) myosin mutations in exons 15–16. In fact, all of them might have some structural impact on the UNC-45B–

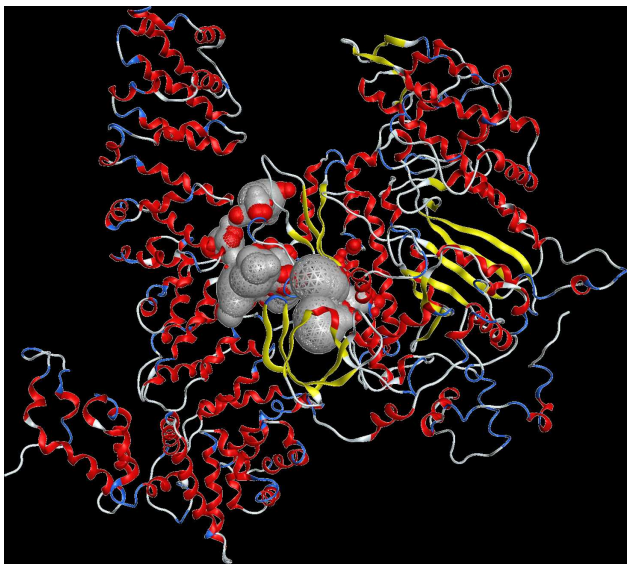

Figure 6

The biggest binding pocket identified at the myosin-UNC-45 interface: the pocket is filled with alpha-spheres. The protein backbone is rendered as a ribbon and colored according to the secondary structure: loop—grey; helix—red; strand—yellow; turn—blue. [Color figure can be viewed in the online issue, which is available at wileyonlinelibrary.com.]

myosin complex, but the mutations in the loop-U and β-sheet would have the most significant contribution due to their stronger interactions with UNC-45. For instance, Asp587Val can strongly influence the interactions with the loop-M lysines, whereas Gly584Arg is in a close contact with Leu598 and could perturb the position of Thr585 too. It may also disturb the myosin β-sheet conformation and thus the total interactions with the loop-M. Similarly, the loop-U mutation Gly571Arg, located at the binding interface between Lys570 and Lys572 that interact with the UNC-45B R19 helix residues, could dramatically affect the complex formation, whereas His576Arg might provoke a conformational change of the loop-U. Met515Arg mutation would have impact on the complex formation due to the close proximity of Met515 to the loop-M and its involvement in hydrophobic interactions with Ile580 (Fig. 5 and Supporting Information Table S2). Based on these results it is reasonable to suggest that there might be UNC-45B mutations too that can provoke cardiomyopathy.

Several dozen potential binding pockets have been found in the complex of UNC-45B and MYH7. The largest one has been identified at the interface between the two proteins (Fig. 6). The analysis of the binding regions showed that both the open and the closed UNC-45B conformations provide relatively large binding sites, for example, an appropriate site for ligand binding has been observed around loop-U and β-sheet of myosin (data not shown). Thus, depending on the cardiomyopathy mutations, several drug targeting ways can be explored and screened for active ligands that could improve the UNC-45B-MYH7 binding of the malfunctioning protein. This might help in discovery of drug candidate for treatment of this disease for individuals harbouring mutations that affect the ability of UNC-45B to optimally bind to myosin.

ACKNOWLEDGMENTS

Acknowledgements are due to Prof. B. Atanasov and Dr. R. Rusev of the Technical University, Sofia, for providing additional computational recourses and the helpful discussion.

REFERENCES

1. Odronitz F, Kollmar M. Drawing the tree of eukaryotic life based on the analysis of 2,269 manually annotated myosins from 328 species. Genome Biol 2007;8:R196.
2. Walsh R, Rutland C, Thomas R, Loughna S. Cardiomyopathy: a systematic review of disease-causing mutations in myosin heavy chain 7 and their phenotypic manifestations. Cardiology 2010;115:49–60.
3. Hutagalung A, Landsverk M, Price M, Epstein H. The UCS family of myosin chaperones. J Cell Sci 2002;115:3983–3989.
4. Wesche S, Arnold M, Jansen RP. The UCS domain protein She4p binds to myosin motor domains and is essential for class I and class V myosin function. Curr Biol 2003;13:715–724.
5. Ni W, Hutagalung AH, Li S, Epstein HF. The myosin-binding UCS domain but not the Hsp90-binding TPR domain of the UNC-45 chaperone is essential for function in *Caenorhabditis elegans*. J Cell Sci 2011;124:3164–3173.
6. Price MG, Landsverk ML, Barral JM, Epstein HF. Two mammalian UNC-45 isoforms are related to distinct cytoskeletal and muscle-specific functions. J Cell Sci 2002;115:4013–4023.
7. Melkani GC, Bodmer R, Ocorr K, Bernstein SI. The UNC-45 chaperone is critical for establishing myosin-based myofibrillar organization and cardiac contractility in the Drosophila heart model. PLoS One 2011;6:e22579.
8. Maron BJ. Hypertrophic cardiomyopathy: a systematic review. JAMA 2002;287:1308–1320.
9. Guo W, Chen D, Fan Z, Epstein HF. Differential turnover of myosin chaperone UNC-45A isoforms increases in metastatic human breast cancer. J Mol Biol 2011;412:365–378.
10. Shi H, Blobel G. UNC-45/CRO1/She4p (UCS) protein forms elongated dimer and joins two myosin heads near their actin binding region. Proc Natl Acad Sci USA 2010;107:21382–21387.
11. Lee CF, Hauenstein AV, Fleming JK, Gasper WC, Engelke V, Sankaran B, Bernstein SI, Huxford T. X-ray crystal structure of the UCS domain-containing UNC-45 myosin chaperone from *Drosophila melanogaster*. Structure 2011;19:397–408.
12. Toi H, Fujimura-Kamada K, Irie K, Takai Y, Todo S, Tanaka K. She4p/Dim1p interacts with the motor domain of unconventional myosins in the budding yeast, *Saccharomyces cerevisiae*. Mol Biol Cell 2003;14:2237–2249.
13. Kaiser CM, Bujalowski PJ, Ma L, Anderson J, Epstein HF, Oberhauser AF. Tracking UNC-45 chaperone-myosin interaction with a titin mechanical reporter. Biophys J 2012;102:2212–2219.
14. Barral JM, Hutagalung AH, Brinker A, Hartl FU, Epstein HF. Role of the myosin assembly protein UNC-45 as a molecular chaperone for myosin. Science 2002;295:669–671.
15. Srikakulam R, Liu L, Winkelmann DA. Unc45b forms a cytosolic complex with Hsp90 and targets the unfolded myosin motor domain. PLoS One 2008;3:e2137.
16. Amorim MJ, Mata J. Rng3, a member of the UCS family of myosin co-chaperones, associates with myosin heavy chains cotranslationally. EMBO Rep 2008;10:186–191.
17. Hoppe T, Cassata G, Barral JM, Springer W, Hutagalung AH, Epstein HF, Baumeister R. Regulation of the myosin-directed chaperone UNC-45 by a novel E3/E4-multiubiquitylation complex in *C. elegans*. Cell 2004;118:337–349.
18. Lord M, Sladewski TE, Pollard TD. Yeast UCS proteins promote actomyosin interactions and limit myosin turnover in cells. Proc Natl Acad Sci USA 2008;105:8014–8019.
19. Lord M, Pollard TD. UCS protein Rng3p activates actin filament gliding by fission yeast myosin-II. J Cell Biol 2004;167:315–325.
20. The Molecular Operating Environment (MOE) Version 2011.10. Chemical Computing Group Inc., 1010 Sherbrooke Street, West, Suite 910, Montreal, Canada H3A 2R7. http://www.chemcomp.com
21. Case DA, Darden TA, IIICheatham TE, Simmerling CL, Wang J, Duke RE, Luo R, Walker RC, Zhang W, Merz KM, Roberts BP, Wang B, Hayik S, Roitberg A, Seabra G, Kolossváry I, Wong KF, Paesani F, Vanicek J, Liu J, Wu X, Brozell SR, Steinbrecher T, Gohlke H, Cai Q, Ye X, Wang J, Hsieh M-J, Cui G, Roe DR, Mathews DH, Seetin MG, Sagui C, Babin V, Luchko T, Gusarov S, Kovalenko A, Kollman PA. AMBER 11. San Francisco: University of California; 2010.
22. Baker NA, Sept D, Joseph S, Holst MJ, McCammon JA. Electrostatics of nanosystems: application to microtubules and the ribosome. Proc Natl Acad Sci USA 2001;98:10037–10041.
23. Humphrey W, Dalke A, Schulten K. VMD—visual molecular dynamics. J Mol Graphics 1996;14:33–38.
24. Tina KG, Bhadra R, Srinivasan N. PIC: protein interactions calculator. Nucleic Acids Res 2007;35:W473–W476.

25. Fernandez-Recio J, Totrov MM, Abagyan RA. Soft protein-protein docking in internal coordinates. Protein Sci 2002;11:280–291. Available at: http://www.molsoft.com/oda.cgi.
26. Fernandez-Recio J, Totrov M, Skorodumov C, Abagyan R. Optimal docking area: a new method for predicting protein-protein interaction sites. Proteins 2005;58:134–143.
27. Ritchie DW, Kozakov D, Vajda S. Accelerating protein-protein docking correlations using a six-dimensional analytic FFT generating function. Bioinformatics 2008;24:1865–1873.
28. De Vries SJ, van Dijk M, Bonvin AMJJ. The HADDOCK web server for data-driven bimolecular docking. Nat Protoc 2010;5:883–897.
29. Genheden S. Are homology models sufficiently good for free-energy simulations? J Chem Inf Model 2012;52:3013–3021.
30. Bryce Group: Computational Biophysics and Drug Design is part of the School of Pharmacy and Pharmaceutical Sciences. Available at: http://www.pharmacy.manchester.ac.uk/bryce/amber.
31. Ryckaert JP, Ciccotti G, Berendsen HJC. Numerical integration of the cartesian equations of motion of a system with constraints: molecular dynamics of n-alkanes. J Comput Phys 1977;23:327–341.
32. Petersen HG. Accuracy and efficiency of the particle-mesh-ewald method. J Chem Phys 1995;103:3668–3679.
33. Suite 2011: Maestro, Version 9.2. New York, NY: Schrödinger, LLC; 2011.
34. Kantardjiev AA, Atanasov BP. PHEPS: web-based pH-dependent electrostatics of proteins server. Nucleic Acid Res 2006;34:W43–W49.
35. Kantardjiev A, Atanasov B. pH-dependent protein electrostatics—hydrogen bond networks perspective. In: Zhongming Zhao , editor. Sequence and genome analysis: methods and applications. 2010. Chap.10, pp155–185.
36. Hodge T, Cope MJ. A myiosin family tree. J Cell Sci 2000;113 Pt 19:3353-3354. Available at: http://jcs.biologists.org/content/113/19/3353.long 2000.
37. Lorenz M, Holmes KC. The actin-myosin interface. Proc Natl Acad Sci USA 2010;107:12529–12534.